Size-Dependent Transition to High-Symmetry Chiral Structures in AgCu, AgCo, AgNi, and AuNi Nanoalloys

ARTICLE *in* NANO LETTERS · OCTOBER 2010

Impact Factor: 13.59 · DOI: 10.1021/nl102588p · Source: PubMed

2 AUTHORS:

Davide Bochicchio
Università degli Studi di Genova
21 PUBLICATIONS **233** CITATIONS
SEE PROFILE

Riccardo Ferrando
Università degli Studi di Genova
234 PUBLICATIONS **8,376** CITATIONS
SEE PROFILE

NANO LETTERS

pubs.acs.org/NanoLett

Size-Dependent Transition to High-Symmetry Chiral Structures in AgCu, AgCo, AgNi, and AuNi Nanoalloys

Davide Bochicchio, and Riccardo Ferrando*

Dipartimento di Fisica and CNISM, Via Dodecaneso 33, Genova, I16146, Italy

ABSTRACT A class of nanomaterials possessing the highest degree of chiral symmetry, the chiral icosahedral symmetry, is found by a combination of global optimization searches and first-principle calculations. These nanomaterials are core−shell nanoalloys with a Cu, Ni, or Co core and a chiral Ag or Au shell of monatomic thickness. The chiral shell is obtained by a transformation of an anti-Mackay icosahedral shell by a concerted rotation of triangular atomic islands which breaks all mirror symmetries. This transformation becomes energetically favorable as the cluster size increases. Other chiral nanoalloys, belonging to a different structural family of C_5 group symmetry, are found in the size range between 100 and 200 atoms. High-symmetry chiral nanoalloys associate strong energetic stability with potential for applications in optics, catalysis, and magnetism.

KEYWORDS Nanoalloys, size-dependent structural transitions, chirality, global optimization, density functional

Nanoalloys, i.e., bi- or multicomponent metallic particles in the size range between 1and100 nm[1] are of great interest for both basic science and technological applications. Applications to magnetism, catalysis and optics stem from the high degree of tunability of the physical and chemical properties of these systems, which is a direct consequence of the great variety of morphologies in which nanoalloys can be produced. Nanoalloys can form crystalline structures, i.e., fragments of bulk crystals, and noncrystalline structures, the most common being icosahedra, decahedra, and polyicosahedra.[2] But variety is not limited to their geometric shape, since the atomic arrangement in nanoalloys can form qualitatively different patterns, such as intermixed (ordered and disordered), core−shell and multishell, and phase-separated patterns (the latter forming the so-called Janus particles[3,4]). This variety of geometries and patterns reflects the complexity of nanoalloy energy landscapes,[5] which renders the theoretical prediction of most stable structures and properties quite challenging.

AgCu, AgCo, AgNi, and AuNi nanoalloys have been recently the subject of notable experimental and theoretical activity,[2,6−11] exploring several different properties and potential applications. Being composed by a ferro- and a non-ferromagnetic metal, the latter (Ag) presenting a sharp surface plasmon resonance (SPR), AgCo and AgNi nanoalloys are studied for their interesting magneto-optical properties. Their SPR frequency can be tuned by changing composition and ordering pattern.[12] Applications to catalysis have been also proposed. AgCo nanoalloys have been employed in the oxygen reduction in alkaline media,[13] whereas AuNi nanoalloy catalysts have been shown to be effective in the steam reforming of *n*-butane.[14] Finally, AgCu nanoalloys have been proposed for the fabrication of Pb-free solder interconnects.[15]

In recent years, great attention has been devoted also to the fabrication and characterization of chiral nanoparticles[16] for applications related to their optical activity. Chiral nanoparticles can absorb differently left and right polarized light,[16] so that they can change the polarization of light from linear to elliptic. This phenomenon is known as circular dichroism. Circular dichroism has been observed in ligand-protected metal clusters and nanoparticles when chiral ligands were used.[17] This discovery has originated an intense research activity devoted to the search and characterization of this novel class of nanomaterials.[16] Moreover, the discovery of chiral nanomaterials has opened new possibilities in fields where enantioselectivity is an issue, such as asymmetric catalysis, and other chiral-related technologies.[18,19]

In this Letter we propose a class of chiral nanomaterials, which are nanoalloys possessing the highest degree of chiral symmetry, i.e., the chiral icosahedral symmetry. Because of their "magic" geometric structure, chiral icosahedra are characterized by a remarkable energetic stability, which is enhanced with incresing size. For small-size AgCu nanoparticles, our calculations find achiral structures consisting of an inner Cu core, in the form of a Mackay icosahedron,[20] surrounded by a monolayer-thick anti-Mackay[21] icosahedral Ag shell (see Figure 1). When size increases, a symmetry-breaking transformation of the Ag shell becomes favorable, so that the cluster loses all its mirror planes while preserving all rotational symmetries of the icosahedron. Chiral icosahedral symmetry has been previously found in viruses,[22] fullerenes,[23] and organometallic compounds.[16,24] A chiral icosahedral gold cage (i.e., a gold empty shell) has been

* To whom correspondence should be addressed, Italyferrando@fisica.unige.it.
Received for review: 07/23/2010
Published on Web: 09/09/2010

DOI: 10.1021/nl102588p | *Nano Lett.* **2010,** *10,* 4211–4216

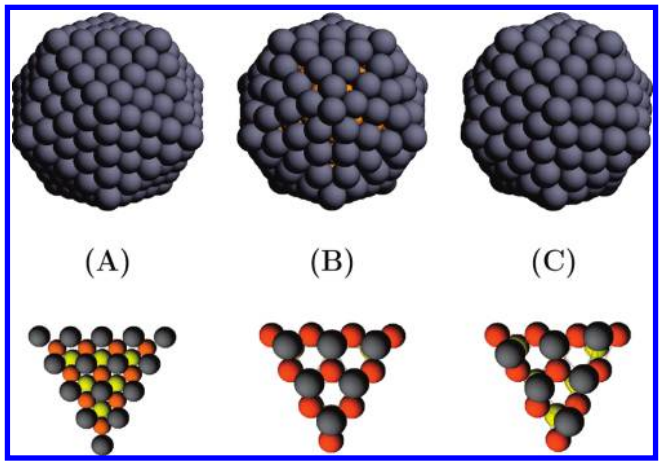

FIGURE 1. Top row: (A) Mackay icosahedron of 309 atoms, for composition $Ag_{162}Cu_{147}$. An external single Ag shell covers a Cu icosahedral core. (B) Anti-Mackay icosahedron of 279 atoms, for composition $Ag_{132}Cu_{147}$. Its Cu core is the same as in the Mackay icosahedron. (C) Chiral icosahedron of 279 atoms, for composition $Ag_{132}Cu_{147}$. Its outer shell is obtained by rotating all triangular Ag islands of the anti-Mackay shell by the same angle so that all mirror symmetries are broken. Neglecting local relaxations, the Cu core preserves the achiral icosahedral symmetry of the previous clusters, while the Ag shell assumes a clearly different structure. Bottom row: The stacking of the three outer atomic shells is shown for the clusters of the top row. Ag atoms are represented by larger spheres (in gray). Two layers of copper atoms are shown. The lowest layer is in yellow (lighter gray). The outer Ag shell is in face-center-cubic-like and hexagonal-close-packed-like stacking for the Mackay and anti-Mackay clusters, respectively. In the anti-Mackay clusters, the Cu atoms of the third layer are covered by the Ag atoms of the external shell. In the chiral cluster, the Ag triangles are rotated so that atoms are displaced from their anti-Mackay sites.

recently proposed for pure Au_{72} clusters.[25] Further calculations have however shown that this cage is not energetically favorable,[26] because there are compact structures of Au_{72} that are lower by about 2.6 eV. On the contrary, our results show that chiral AgCu icosahedra are clearly favorable from the energetic point of view for sizes above 500 atoms. We discuss the driving forces for the transformation to chiral icosahedral structures and we find that their stability is caused by factors of quite general character. This generality is confirmed by the behavior of AgNi, AgCo, and AuNi nanoalloys, for which we find that the transformation mechanism is even more effective than in AgCu. Finally, we single out also nonicosahedral high-symmetry chiral structures belonging to different structural motifs.

Our computational methodology consists of a combination of global optimization searches within a semiempirical atom−atom potential and of density-functional (DF) calculations. The atom−atom potential is of the same form used in refs 2, 6, and 27. In the case of AgCu, this potential has been refitted in order to improve its agreement with DF results for what concerns the structures of small nanoalloys (sizes up to 55 atoms). The refitted potential (potential P1 in the following) has then been tested against DF calculations and the old parametrization (potential P2) for selected structures of larger sizes, up to about 300 atoms (above these sizes, DF calculations become extremely cumbersome). The DF calculations have been carried out using the PWscf (Plane-Wave Self-Consistent Field) code,[28] with the PBE exchange-correlation (xc) functional[29] and ultrasoft pseudopotentials. The kinetic energy cutoff is 40 Ryd for the energy and 160 Ryd for the density for all calculations. A large simulation cell has been chosen so that the distance between the closest atoms of different periodic images is at least of 10 Å. A Gaussian smearing technique (smearing parameter of 0.002 Ryd) has been applied. Form and parameters of P1 and P2, together with a thorough comparison with the results of DF calculations, are given in the Supporting Information. Here we note that the agreement with DF results is very good.

Global optimization of large clusters (300 atoms and more) is presently a challenge already for single-component systems.[30] Nanoalloys are even more difficult because of their more complex energy landscape, presenting a much larger number of possible structures for a given size.[1] For this reason, we have developed a specifically tailored global optimization algorithm to increase the efficiency of the search in systems, such as AgCu, that present a quite strong tendency to unmix in the bulk phase, thus being likely for developing core−shell or phase-separated arrangements of nanoparticles. This algorithm is a two-temperature modification of the basin-hopping algorithm,[31] which uses two kinds of elementary moves: (a) short molecular-dynamics or shake moves;[32] (b) moves in which the positions of atoms of different species are exchanged. The exchanges are specifically tailored for this system, so that it is more likely to attempt exchanging either low-coordination Cu atoms with high-coordination Ag atoms or Ag and Cu atoms that have nearest neighbors of both species. Moves (a) and (b) are accepted according to the Metropolis rule but with two different temperatures, a high temperature (in the range 2000−3000 K) for move (a) and a low temperature (100−500 K) for move (b). This algorithm improves the efficiency of the search in this system by orders of magnitudes compared to the standard basin-hopping scheme with random exchanges.

Let us first discuss the results of the global optimization of AgCu nanoparticles. In this case, core−shell arrangements with a Cu core and Ag shell are expected, as follows from experiments and calculations.[2,4,33] We consider magic sizes for icosahedral structures. Magic numbers of Mackay icosahedra are given by the formula $N_M(k) = (10k^3 - 15k^2 + 11k - 3)/3$, where $k \geq 1$ is the number of shells, so that one obtains $N_M = 1, 13, 55, 147, 309, 561, 923, \ldots$. A different set of magic numbers can be obtained by substituting the outer shell of a Mackay icosahedron by an anti-Mackay shell. This corresponds to putting the atoms of the outer shell on hexagonal-close-packed-like instead of face-centered-cubic-like sites of the substrate (see Figure 1). In this way, a smaller number of atoms can be accommodated, so that the magic numbers for anti-Mackay icosahedra are $N_{aM}(k) = N_M(k) - 10(k-2)$, $k \geq 3$, giving the sequence $N_{aM} = 45, 127,$

DOI: 10.1021/nl102588p | *Nano Lett.* **2010,** *10,* 4211–4216

FIGURE 2. Lowest-energy isomers belonging to the competing structural motifs in $Ag_{72}Cu_{55}$. From left to right, anti-Mackay icosahedron, incomplete Mackay icosahedron (20 more Ag atoms would be necessary to complete the outer shell, which is also somewhat reconstructed), and tetraIh.

279, 521, 873, ..., with compositions $Ag_{32}Cu_{13}$, $Ag_{72}Cu_{55}$, $Ag_{132}Cu_{147}$, $Ag_{212}Cu_{309}$, $Ag_{312}Cu_{561}$ for perfect core−shell structures with an Ag shell of monatomic thickness.

From the energetic point of view, the anti-Mackay shell is usually unfavorable in single-component clusters, so that an incomplete Mackay shell is more stable even for anti-Mackay magic numbers (in 45-atom pure Cu or Ag clusters, incomplete Mackay shells win by 3.52 and 3.06 eV, respectively, according to our DF calculations). But for binary AgCu clusters the situation may be different, because the lattice mismatch between the components (13% in favor of Ag) may favor an outer shell with fewer Ag atoms, such as the anti-Mackay shell.

Our global optimization results for $Ag_{72}Cu_{55}$ confirm this hypothesis. For this nanoalloy, we find three competing motifs (see Figure 2): the anti-Mackay icosahedron, the incomplete Mackay icosahedron, and an incomplete polyicosahedron. The last structure (named tetraIh in the following) is made of four interpenetrating icosahedra of 55 atoms and is completed for size 128; therefore one atom (a vertex atom) is missing. We note that the tetraIh is a different type of polyicosahedron than those found in ref 2 because in that case the polyicosahedra were made of smaller interpenetrating icosahedra of 13 atoms. The anti-Mackay structure is the lowest in energy, followed by the tetraIh, which is higher by about 0.7 eV, and by the Mackay structure, higher by more than 2 eV, as can be seen in Table 1, where P1, P2, and DF results are reported.

At the next magic size and composition of anti-Mackay icosahedra, which is $Ag_{132}Cu_{147}$, a further structural motif comes into play, the chiral icosahedron (see Figure 1). For $Ag_{72}Cu_{55}$ this structure is not even a stable local minimum, according to both atom−atom potential and DF calculations. According to DF and P1 results, for $Ag_{132}Cu_{147}$ the chiral structure is not the global minimum, but it is separated from the anti-Mackay achiral structure by a quite small amount of energy, less than 0.5 eV. Incomplete Mackay icosahedra are much higher in energy (more than 7 eV). In the chiral structure, the external Ag shell is transformed with respect to the anti-Mackay structure, assuming the shape of a *snub icosahedron*.[22,34]

Increasing size to $Ag_{212}Cu_{309}$, the situation is reversed. The global optimization searches single out the chiral structure as the lowest in energy, while the achiral anti-Mackay structure is not even a stable local minimum, according to P1 results. The anti-Mackay structure becomes a stable local minimum if the 12 vertex Ag atoms are eliminated, i.e., for Ag_{200} Cu_{309}. However, also in this case, the chiral structure is considerably more favorable, being lower in energy by about 1.7 eV. The transition to the chiral structure is confirmed by global optimization searches for the 873-atom cluster $Ag_{312}Cu_{561}$, which locate the chiral icosahedron as the lowest energy structure, while the anti-Mackay structure is again unstable. The energy difference between these structures clearly increases with increasing size.

TABLE 1. Energetics of AgCu Nanoalloys[a]

system	structure	DF	P1	P2
$Ag_{72}Cu_{55}$	anti-Mackay icosahedron	0.000	0.000	0.000
	tetraih	0.644	0.744	1.184
	incomplete Mackay icosahedron	2.013	2.604	2.952
	chiral icosahedron	not stable	not stable	not stable
$Ag_{132}Cu_{147}$	anti-Mackay icosahedron	0.000	0.000	0.132
	chiral icosahedron	0.430	0.072	0.000
	incomplete Mackay icosahedron	7.083	7.943	7.599
$Ag_{212}Cu_{309}$	chiral icosahedron		0.000	0.000
	anti-Mackay icosahedron		not stable	2.171
$Ag_{200}Cu_{309}$	chiral icosahedron		0.000	0.000
	anti-Mackay icosahedron		1.666	1.718
$Ag_{312}Cu_{561}$	chiral icosahedron		0.000	0.000
	anti-Mackay icosahedron		not stable	6.448

[a] In all cases, the zero of the energy scale is the energy of the lowest isomer. All data are in eV. Results of DF calculations and of two different parametrizations of the atom−atom potential (P1 and P2) are reported.

If we consider the potential parametrization P2,[2,6] we find that its overall agreement with DF calculations is good, as follows from the results in Table 1 and from the more complete data reported in the Supporting Information. However, at variance with DF calculations, the transition from the anti-Mackay to the chiral icosahedron already occurs for $Ag_{132}Cu_{147}$, where the two structures are almost degenerate. For $Ag_{212}Cu_{309}$ and $Ag_{312}Cu_{561}$ the anti-Mackay is higher by more than 2 and 6 eV, respectively.

What is the driving force for the transition to chiral icosahedral structures? The mechanism undelying the transition can be directly related to the geometric structures of achiral and chiral shells and rationalized in terms of simple bond-counting arguments. The transformation of an achiral anti-Mackay shell into a chiral shell takes place via the concerted rotation of the triangular Ag islands that cover the facets of the Cu core (see Figure 1) by the same angle (close to 19.5°[35]). This rotation has two effects: (a) Ag atoms are slightly displaced from their anti-Mackay equilibrium sites on the facet and (b) new Ag−Ag nearest-neighbor bonds are formed along the facets edges, as shown in Figure 3. In $Ag_{132}Cu_{147}$, two new nearest-neighbor bonds are formed at each edge, but they are quite stretched, since the distance between the new neighbors is 3.17 Å (recall that the equilibrium distance in bulk Ag is of 2.89 Å). The situation

DOI: 10.1021/nl102588p | *Nano Lett.* **2010,** *10,* 4211–4216

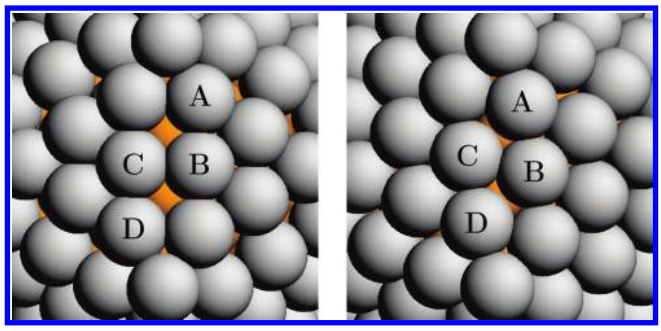

FIGURE 3. Atomic configurations along facet edges in $Ag_{132}Cu_{147}$ for the anti-Mackay achiral structure (left) and for the chiral icosahedron (right). The transformation to the chiral icosahedron creates two new nearest-neighbor A−C and B−D bonds. These bonds are however quite stretched in this case. The lengths of these additional bonds along edges improve in larger size chiral icosahedra.

TABLE 2. Energetics of AgNi, AgCo, and AuNi Nanoalloys According to DF Calculations[a]

system	ΔE
$Ag_{72}Ni_{55}$	0.274
$Ag_{132}Ni_{147}$	3.43
$Ag_{72}Co_{55}$	0.006
$Au_{72}Ni_{55}$	0.074

[a] ΔE is the energy difference (in eV) between the achiral anti-Mackay structure and the chiral icosahedral structure.

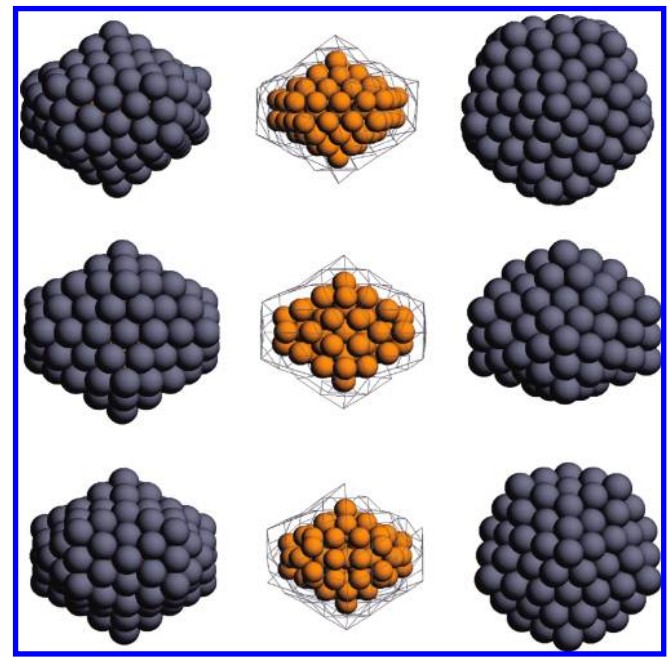

FIGURE 4. (top row) Chiral structure of $Ag_{107}Cu_{85}$. (middle row) Achiral pentalh structure of $Ag_{90}Cu_{56}$. (bottom row) Achiral eptalh structure of $Ag_{102}Cu_{75}$. From left to right, for all structures the first and second snapshots are side views (the second showing the structure of the inner Cu core), and the third is a top view.

improves with increasing size. For $Ag_{212}Cu_{309}$, three new bonds per edge are formed. They are still stretched, but by a smaller amount, since two of them are of 3.01 Å and the third is of 3.13 Å. Finally, for $Ag_{312}Cu_{561}$ four bonds per edge are formed, two of 2.91 Å and two of 3.03 Å, thus close to the optimal length. For $Ag_{132}Cu_{147}$, the energy gain due to the new stretched bonds is overcompensated by the loss due to the displacement of Ag atoms from their anti-Mackay sites. For larger sizes, the energy gain of the new bonds prevails, so that the chiral structure becomes favorable. We note in passing that the chiral shell is more compact than the anti-Mackay shell, and therefore it would benefit from a somewhat smaller inner core to achieve a more effective strain release.

Since the transformation to the chiral icosahedron is driven by factors that are simply related to the geometry of the structure, it is natural to check whether the same transformation takes place in nanoalloys that share some common crucial features with AgCu. These features are (a) atomic size mismatch between the components, (b) tendency to surface segregation of the "big" atomic species, and (c) weak tendency to intermixing of the components. (b) and (c) are driving forces for the formation of core−shell structures,[1] and (a) favors anti-Mackay over Mackay icosahedral shells. Among the systems presenting these features there are AgNi, AgCo, and AuNi with either Ag or Au playing the role of "big" atoms. As follows from the DF data reported in Table 2, the transition from anti-Mackay to chiral icosahedra is even more favored in these systems than in AgCu. In fact, the transition is accomplished already for size 127, even though energy differences between anti-Mackay and chiral structures are quite small, being of a fraction of electronvolt. Energy differences in favor of the chiral icosahedron are however expected to increase with nanoparticle size, as seen in the case of AgCu and verified also for AgNi. In fact, for Ag_{132} Ni_{147}, the energy difference in favor of the chiral structure is more than 3 eV.

The enhanced stability of chiral icosahedra in AgNi, AgCo, and AuNi can be attributed to the smaller size of Ni and Co nanoparticle cores compared to Cu cores. Since the chiral shell is more contracted than the anti-Mackay shell, a smaller core favors the transformation. This is supported also by the fact that in a further system, AuCo, the transition is not yet accomplished for size 127. Therefore, for size 127, the smallest core atom (Ni) stabilizes the chiral structure for both Au and Ag shells, whereas the intermediate-size core atom (Co) stabilizes only the Ag shell. Finally, the biggest core atom (Cu) stabilizes the Ag chiral shell only for sizes above 500 atoms. Here we do not consider AuCu, because it is a qualitatively different system due to the strong tendency to intermixing of these elements in the bulk phase.

Our global optimization searches of AgCu nanoalloys have singled out also another family of chiral structures that belong to the C_5 symmetry group, i.e., a group with a single 5-fold rotation axis. Structures of this family have been found for $Ag_{67}Cu_{39}$ and $Ag_{107}Cu_{85}$. The latter is shown in the top row of Figure 4, and it has a one-layer Ag shell. The inner Cu core can be seen as either an icosahedral fragment or a capped decahedron, and if we neglect small local relaxations, it is achiral. Therefore, also in these C_5 structures

DOI: 10.1021/nl102588p | *Nano Lett.* **2010,** *10,* 4211–4216

chirality is mostly due to a specific arrangement of the shell atoms. $Ag_{107}Cu_{85}$ is of size 192, which is the geometric magic size of a Marks decahedron.[36] We have compared the Marks decahedron and the C_5 chiral structure, finding that the latter is lower in energy by several electronvolts.

In order to check the stability of chiral core−shell structures at finite temperatures, we have studied the melting of the chiral icosahedron $Ag_{212}Cu_{309}$ by molecular dynamics simulations, in which the temperature has been increased by 1 K/ns. This heating rate is sufficient for describing correctly the melting of AgCu nanoparticles.[37] Potential P1 has been employed. The simulations show that the cluster retains its low-temperature shape up to about 640 K, simply vibrating in the basin of the global minimum structure. Between 640 and 700 K, the external Ag shell is still perfectly chiral for most of the time, but the first signs of disordering processes begin to appear, because sometimes a single vertex atom escapes from its position and diffuses shortly on the cluster surface, before being retrapped again at the vertex. Above 700 K, more evident surface melting phenomena take place. One or two diffusing Ag atoms are always found, but the external shell still retains its overall chiral shape, with one or two atomic vacancies, that are most likely (but not always) placed at vertices. The structure is identifiable as a defective chiral icosahedron. For temperatures around 800 K, exchanges between silver and copper atoms begin to take place. The perfect core−shell arrangement is lost. From this temperature on, the structure is no more identifiable as a defective chiral icosahedron, even though its copper core is still icosahedral (with defects) and parts of the shell retain the typical arrangement of the chiral structure. The overall melting of the cluster takes place in the range 920−960 K, where a neat jump in the caloric curve is observed. The surface melting of the outer shell of chiral icosahedral $Ag_{212}Cu_{309}$ therefore occurs at temperatures that are in the same range as the overall melting of pure Ag icosahedra of comparable size.[37]

We note also that preliminary simulations of AgCu clusters on MgO(001) show that structures of the chiral icosahedral family can be formed, for example for $Ag_{100}Cu_{100}$. These structures resemble a half chiral icosahedron, as can be qualitatively understood considering the Wulff−Kaischew construction.[38]

Finally, also high-symmetry achiral structures of remarkable stability have been found. These structures are polyicosahedra, but made of interpenetrating icosahedra of 55 atoms, as the one shown in Figure 2. We find a perfect core−shell tetraIh for size 128, and composition $Ag_{70}Cu_{58}$. A structure made of five icosahedra, the pentaIh, is found for $Ag_{90}Cu_{56}$, while one made of seven icosahedra, the eptaIh, is found for $Ag_{102}Cu_{75}$ (see Figure 4). The tetraih and the pentaIh are of high symmetry, tetrahedral and D_{5h}, respectively. The pentaIh has been compared to the Mackay icosahedron of magic size 147, which presents a perfect core−shell arrangement for composition $Ag_{92}Cu_{55}$. Size and composition are not magic for the pentaIh, with an excess of two Ag atoms and one Cu atom missing. For this reason, one Ag atom must be placed inside the cluster (replacing the missing Cu atom), and another adsorbed on the cluster surface, with low coordination. However, the pentaIh structure is lower in energy than the Mackay icosahedron according to both atom−atom potential and DF calculations, by 0.13 eV, 1.36, and 0.35 eV for P1 potential, P2 potential, and DF calculations, respectively.

In conclusion, our calculations predict the stability of a class of high-symmetry chiral nanomaterials. Their notable energetic stability, which derives from their "magic" geometry, renders them suitable for practical applications. Silver-contaning chiral clusters are very promising for applications in optics, because they are expected to associate the sharp SPR of silver together with the optical activity induced by the chiral geometry. For Co- and Ni-containing nanoparticles, a SPR-enhanced magneto-optical response can be expected. Finally, these chiral clusters are likely to present interesting catalytic properties, both because of their chirality and for the peculiar atomic configuration of their outer shell, which has no counterpart in bulk crystal surfaces and in achiral nanoparticles.

Acknowledgment. The authors acknowledge support from Italian MIUR for the PRIN Project No. 2007LN873M_003, from CINECA and CNR-INFM for the project "Properties of Exotic Phases of Metal-on-Oxide Nanodots", and from the COST Action MP0903 "Nanoalloys as Advanced Materials: From Structure to Properties and Applications".

Supporting Information Available. Details of the computational methodology and of the model potential parametrization and supplementary data on the energetics of cluster structures. This material is available free of charge via the Internet at http://pubs.acs.org.

REFERENCES AND NOTES

(1) Ferrando, R.; Jellinek, J.; Johnston, R. L. *Chem. Rev. (Washington, DC, U.S.)* **2008**, *108*, 845.
(2) Rossi, G.; Rapallo, A.; Mottet, C.; Fortunelli, A.; Baletto, F.; Ferrando, R. *Phys. Rev. Lett.* **2004**, *93*, 105503.
(3) Parsina, I.; Baletto, F. *J. Phys. Chem. C* **2010**, *114*, 1504.
(4) Langlois, C. T.; Oikawa, T.; Bayle-Guillemaud, P.; Ricolleau, C. *J. Nanopart. Res.* **2008**, *10*, 997.
(5) Wales, D. J. *Energy Landscapes*; Cambridge University Press: Cambridge, 2003.
(6) Baletto, F.; Mottet, C.; Ferrando, R. *Phys. Rev. Lett.* **2003**, *90*, 135504.
(7) Ortigoza, M. A.; Rahman, T. S. *Phys. Rev. B* **2008**, *77*, 195404.
(8) Delfour, L.; Creuze, J.; Legrand, B. *Phys. Rev. Lett.* **2009**, *103*, 205701.
(9) Hoz, J. M. M. D. L.; Tovar, R. C.; Balbuena, P. B. *Mol. Simul.* **2009**, *35*, 785.
(10) Wang, L. L.; Johnson, D. D. *J. Am. Chem. Soc.* **2009**, *39*, 14023.
(11) Kilimis, D. A.; Papageorgiou, D. G. *Eur. Phys. J. D* **2010**, *58*, 189.
(12) Gaudry, M.; Cottancin, E.; Pellarin, M.; Lermé, J.; Arnaud, L.; Huntzinger, J. R.; Vialle, J. L.; Broyer, M.; Rousset, J. L.; Treilleux, M.; Mélinon, P. *Phys. Rev. B* **2003**, *67*, 155409.
(13) Lima, F. H. B.; de Castro, J. F. R.; Ticianelli, E. A. *J. Power Sources* **2006**, *161*, 806.
(14) Molenbroek, A. M.; Norskov, J. K.; Clausen, B. S. *J. Phys. Chem. B* **2001**, *105*, 5450.

DOI: 10.1021/nl102588p | *Nano Lett.* **2010,** *10,* 4211–4216

(15) Kim, S. J.; Stach, E. A.; Handwerker, C. A. *Appl. Phys. Lett.* **2010**, *96*, 144101.
(16) Noguez, C.; Garzon, I. L. *Chem. Soc. Rev.* **2009**, *38*, 757.
(17) Schaaff, T. G.; Whetten, R. L. *J. Phys. Chem. B* **2000**, *104*, 2630.
(18) López-Lozano, X.; Pérez, L. A.; Garzón, I. L. *Phys. Rev. Lett.* **2006**, 233401.
(19) Kitaev, V. *J. Mater. Chem.* **2008**, *18*, 4745.
(20) Mackay, A. L. *Acta Crystallogr.* **1962**, *15*, 916.
(21) Harris, I. A.; Kidwell, L. S.; Northby, J. A. *Phys. Rev. Lett.* **1984**, *53*, 2390.
(22) Longuet-Higgins, M. S. *Proc. R. Soc. London, Ser. A* **2009**, *465*, 477.
(23) Terrones, M.; Terrones, G.; Terrones, H. *Struct. Chem.* **2002**, *13*, 373.
(24) Vollet, J.; Hartig, J. R.; Schnöckel, H. *Angew. Chem., Int. Ed.* **2004**, *43*, 3186.
(25) Karttunen, A. J.; Linnolahti, M.; Pakkanen, T. A.; Pyykko, P. *Chem. Commun.* **2008**, 465.
(26) Johansson, M. P.; Vaara, J.; Sundholm, D. *J. Phys. Chem. C* **2008**, *112*, 19311.
(27) Rossi, G.; Schiappelli, G.; Ferrando, R. *J. Comput. Theor. Nanosci.* **2009**, *6*, 1.
(28) Giannozzi, P.; et al. *J. Phys.: Condens. Matter* **2009**, *21*, 395502.
(29) Perdew, J. P.; Burke, K.; Ernzerhof, M. *Phys. Rev. Lett.* **1996**, *77*, 3865.
(30) Bao, K.; Goedecker, S.; Koga, K.; Lançon, F.; Neelov, A. *Phys. Rev. B* **2009**, *79*, 041405.
(31) Wales, D. J.; Doye, J. P. K. *J. Phys. Chem. A* **1997**, *101*, 511.
(32) Rossi, G.; Ferrando, R. *J. Phys.: Condens. Matter* **2009**, *9*, 084208.
(33) Langlois, C.; Alloyeau, D.; Bouar, Y. L.; Loiseau, A.; Oikawa, T.; Mottet, C.; Ricolleau, C. *Faraday Discuss.* **2008**, *138*, 375.
(34) Coxeter, H. S. M.; Longuet-Higgins, M.; Miller, J. C. P. *Philos. Trans. R. Soc., A* **1954**, *246*, 501.
(35) Messer, P. W. *Discrete Comput. Geom.* **2002**, *27*, 353.
(36) Marks, L. D. *Rep. Prog. Phys.* **1994**, *57*, 603.
(37) Mottet, C.; Rossi, G.; Baletto, F.; Ferrando, R. *Phys. Rev. Lett.* **2005**, *95*, 035501.
(38) See for example: Henry, C. R. *Prog. Surf. Sci.* **2005**, *80*, 92.

DOI: 10.1021/nl102588p | *Nano Lett.* **2010,** *10,* 4211–4216